Final design of SITELLE, a wide-field imaging Fourier transform spectrometer for the Canada-France-Hawaii telescope

F. Grandmont*[a], L. Drissen[b], Julie Mandar[a], S. Thibault[b], Marc Baril[c] and the SITELLE Team

[a]ABB, 585 Boul. Charest est, Suite 300, Québec, Qc, Canada G1K 9H4
[b]Dépt. de physique, de génie physique et d'optique, Université Laval, Québec, Qc, Canada G1V 0A6 and Centre de recherche en astrophysique du Québec (CRAQ)
[c] Canada-France-Hawaii Telescope Corporation, Mamalaoha Highway, Kamuela, HI, 96743 USA

ABSTRACT

We report here on the current status of SITELLE, an imaging Fourier transform spectrometer to be installed on the Canada-France Hawaii Telescope in 2013. SITELLE is an Integral Field Unit (IFU) spectrograph capable of obtaining the visible (350 nm – 900 nm) spectrum of every pixel of a 2k x 2k CCD imaging a field of view of 11 x 11 arcminutes, with 100% spatial coverage and a spectral resolution ranging from R = 1 (deep panchromatic image) to R > 10^4 (for gas dynamics). SITELLE will cover a field of view 100 to 1000 times larger than traditional IFUs, such as GMOS-IFU on Gemini or the upcoming MUSE on the VLT. SITELLE follows on the legacy of BEAR, an imaging conversion of the CFHT FTS and the direct successor of SpIOMM, a similar instrument attached to the 1.6-m telescope of the Observatoire du Mont-Mégantic in Québec. SITELLE will be used to study the structure and kinematics of HII regions and ejecta around evolved stars in the Milky Way, emission-line stars in clusters, abundances in nearby gas-rich galaxies, and the star formation rate in distant galaxies.

Keywords: Fourier transform spectroscopy, hyperspectral imagery, Integral Field Unit

1. INTRODUCTION

SITELLE (**S**pectromètre **I**mageur à **T**ransformée de Fourier pour l'**E**tude en **L**ong et en **L**arge de raies d'**E**mission, or Imaging FTS for the study of emission lines) has been approved as a guest instrument for the Canada-France-Hawaii telescope (CFHT). Funded by the Canada Foundation for Innovation with additional financial participation by the CFHT, Université Laval, ABB and e2v, SITELLE is an imaging Fourier transform spectrometer (FTS) capable of obtaining spectra in selected wavebands in the visible (from 350 to 850 nm) of every light source in an 11 x 11 arcminute field of view with a spatial sampling of 0.32". Its spectral resolution is variable, depending on the requirement of the observer, from R = 1 (broad-band image) to R in excess of 10^4. The spatial resolution is limited by the seeing, resulting in ~ 10^6 different spectra. The dual output interferometer configuration of SITELLE ensures that virtually every photons collected by the telescope reaches the detector and is analyzed; a by-product of the spectral data cubes is therefore a very deep panchromatic image of the targets. SITELLE's design is based on that of a previous prototype, SpIOMM, attached to the 1.6-m telescope of the Observatoire du Mont Mégantic (Drissen et al., these proceedings). SpIOMM and SITELLE's early development phase was presented by Grandmont, Drissen and collaborators [1-5].

Despite its name and acronym, SITELLE will also be able to perform absorption line studies, like the vast majority of FTS in astronomy, planetary space missions or remote sensing devices.

Most of the design and construction work is being performed by ABB Analytical , a Québec-based company specialized in Fourier transform spectrometers and optical sensors. Science lead, optical design and its integration are done at

*frederic.j.grandmont@ca.abb.com; phone 1 418 877 2944 x-318; fax 1 418 266 1422

Université Laval, the mechanical design and fabrication of the input and output ports at Université de Montréal, while CFHT takes charge of the detectors' enclosure and cooling system.

The advantages and disadvantages of the imaging FTS technique, as well as the relative merit of different approaches to 3-D imagery are discussed by Ridgway & Brault [6], Bennett [7] and, more recently, by Maillard et al.[8].

2. SCIENCE DRIVERS AND INTRUMENT REQUIREMENTS

2.1 Science drivers

While the number of scientific programs for this type of instrument is potentially huge (from the study of individual stars in local star clusters to the search for high-redshift Ly-α emitters), we have chosen a series of typical projects to illustrate its scientific potential by advocating the enormous benefits provided by a systematic, complete 3D mapping of extended emission-line sources. The main science drivers for SITELLE are very similar to those of SpIOMM, a prototype imaging FTS attached to the Observatoire du Mont Mégantic's 1.6-m telescope (see Drissen et al., these proceedings): the study of physical characteristics (temperature, density, kinematics) of nebulae surrounding evolved stars, supernova remnants and the diffuse interstellar gas in the Milky way galaxy; abundance gradients and kinematics of nearby galaxies to understand their evolution; distant galaxies. The much higher throughput and efficiency of SITELLE at CFHT will allow us to map fainter emission lines, to broaden the study of galaxies to the absorption lines due to the presence of an old stellar population, and to extend the study of galaxies to much higher redshift in order to study, for example, the star-formation rate across the Universe.

Our team has learned a lot from the development of SpIOMM and especially from its use on a regular basis at a telescope. All the potential improvements we have identified will be fully integrated in SITELLE. In particular, we expect:

- A much better sensitivity in the near-UV, mainly because of significant improvements in the interferometer's performances.
- More sensitive CCDs, mostly because of a significant readout noise reduction (from 10e to 3e).
- Much lower dead time between exposures (2 seconds instead of 7), a combination of CCD readout and interferometer performances.

2.2 Instrument requirements

The science requirements have defined the following technical requirements of SITELLE which have been used in the design of the instrument:

- Wavelength range - In the local universe, the [OII] 372.7 nm doublet defines the short wavelength requirement. It is used to measure the oxygen abundance in ionized nebulae and the ratio of its two components is an excellent indicator of the electron density in the interstellar medium. Many factors conspire to make this line a real challenge for an Imaging FTS, and in particular the stringent constraints it imposes on the quality of the optical surfaces within the interferometer (mirrors and beamsplitter) as well as the precision of the step-scan and servo mechanisms to which the modulation efficiency is particularly sensitive at short wavelengths. The long wavelength limit is defined by the Ca triplet at 849.8 nm, 854.2 nm and 866.2 nm, which characterizes the old stellar population in galaxies. In the case of the high redshift objects, the wavelength range accessible with the instrument defines the redshift range in which the Lyα line can be detected. The above-mentioned limits (370 – 870 nm) set this range to $2.0 < z < 6.15$.
- Spectral resolution – The minimum resolution required for the analysis of the ionized nebula in the Milky way and other galaxies is set by the necessity to separate the [SII] 671.7 / 673.1 nm doublet, the Hα 656.3 nm from its [NII] 654.8 nm and 658.4 nm neighbors, and Hγ 434.1 nm from [OIII] 436.3 nm. This implies a minimum value of R = 1000 over the entire wavelength range. However, kinematics of HII regions and the studies of stars in clusters impose a more stringent requirement of $R = 10^4$.

- Field of view – For the study of extended HII regions in the Milky Way, nearby galaxies and the high-redshift Universe, reasonable amounts of observing time require a FOV > 10 arcminutes, which set the constraints for SITELLE. A larger FOV is always welcome but leads to complexity increases that are not linear with the field size beyond this point. The specified value appears as a suit spot considering the available budget.
- Spatial resolution – Most of the projects presented here put the emphasis on the wide field observation of extended, diffuse objects and not on the spatial resolution. However, observations of individual stars in clusters and distant galaxies require that the pixel size be no larger than the typical seeing, 0.6 arcsec. The panchromatic image quality (350 – 900 nm) should be no worse than one arcsec.
- Sensitivity – Two of the most stringent constraints in terms of sensitivity, from the science case, are the ability of SITELLE to detect the faint [OIII] 436.3 line, which is not always detected in HII regions, and its capacity to detect Lyman apha emitters down to a flux of 4.3×10^{-17} ergs s^{-1} cm^{-2} (5 sigma detection) in a reasonable integration time (less than 4 hours).
- High observing efficiency – The readout time, combined with the displacement time of the interferometer between OPD sampling position should be a small fraction of the total on-target exposure time. Considering the read time attainable with low read noise (~3 electrons) on modern CCD, a 2 second interferometer displacement time seems like an acceptable upper limit. For example, 500 images cube acquired over a few hours would limit the dead time to around 15 minutes.
- Autonomy – CFHT now requires that all its instruments be remotely operated for periods of at least one week without direct human intervention.

3. SITELLE DESIGN

3.1 Optical design

The design of an IFTS with such emphasis on the imaging/throughput aspect obviously starts by attempting to meet the FOV and image quality requirement over the desired wavelength range simultaneously. This is a challenging task compared to similar astronomical instruments. On one side, wide field camera systems can typically suffer from chromatic aberrations to some degree since band pass filters are typically used and allow for a focus correction. On the other side, Integral field unit spectrometers will typically image a much smaller FOV than SITELLE or, if not, allow for very coarse spatial sampling of it (hence poor image quality). All images acquired with an IFTS are meant to be panchromatic and take full advantage of all the available detector pixels for imagery. Band pass filters can still be used but primarily to reduce the photon noise in the spectra or the number of images required for cube completion and not specifically to improve image quality.

The optical design process can be carried out almost independently from the interferometer design as the latter typically adds only reflecting or transmissive flat interfaces which effect on the optical performances are often negligible. The IFTS configuration practically bring one additional requirements to the optical design which is the need to dispose of a collimated beam section of sufficient length to place the interferometer. This latter is ideally centered around a pupil image in the collimated section where the beam envelope is the smallest.

The input/output optical design's intent was to converge to a solution that provided the largest FOV without compromising the wavelength range and image quality threshold as dictated by the science requirements. The pupil size of the collimated section (90mm) was set by the desire to limit as much as possible the size of the interferometer optics which require the high flatness requirement and must be moved by the OPD scanning mechanism. For a given FOV, reducing the interferometer pupil size increases the divergence before the camera lens and further complicates its design. A parametric model of the overall optical design including a metrology channel was established and demonstrated that the dimension of the interferometer had a minima near a pupil of 90 mm.

The final design, which is composed of a triplet for input optics and six lenses in the output optics (see Figure 1), allows an unvignetted circular field of view of 5.5 arcminute radius with a full fov of 11' x 11' (0.32" per pixel) with a 15% vignetting in the corners of the field. The image quality specification is fully met with this final design.

The large number of lenses in the optical path (18 surfaces) brings the challenge of finding suitable anti-reflection coatings which will not significantly attenuate the light.

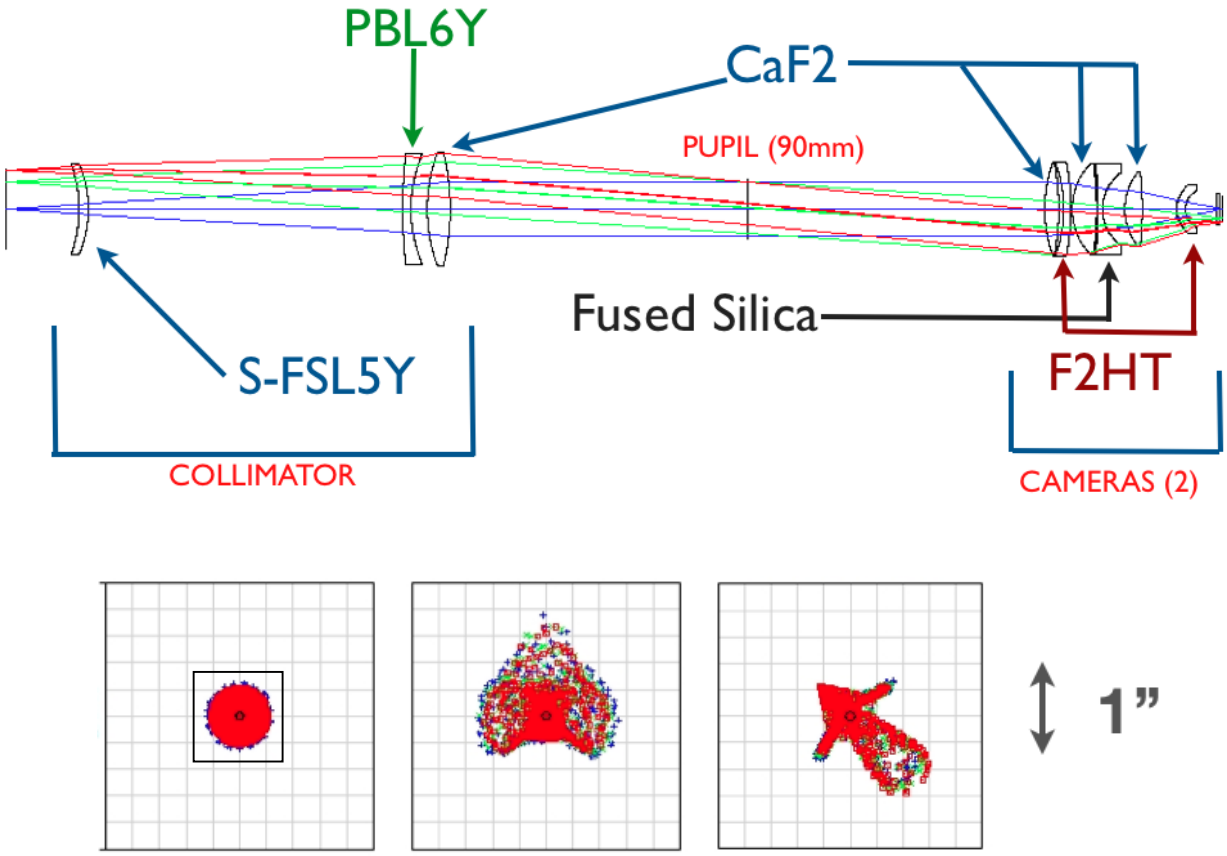

Fig. 1 - SITELLE optical design (top) and resulting spot diagrams (bottom) of the 650 - 680 nm wavelength range in the center of the field (left), 5.5' from the center (edge center) and corners of the field (right).

3.2 Interferometer design

The interferometer design is largely driven by the desire to obtain high efficiency at near UV wavelengths. A very small number of interferometers are found to have operated in the UV regime in the general literature and there is a good reason for it. The modulation efficiency of any interferometer shows an exponential-like decline in performance as we move toward shorter wavelengths. Many factors affect the modulation efficiency in such a way:

1- Wavefront errors between the two recombining beams at the beamsplitter 2nd pass;

2- Tilt between the two recombining beams at the beamsplitter 2nd pass;

3- Shear between the two recombining beams factored by the beam divergence determined by the detector size;

4- OPD jitters encountered during exposure of the detector.

The first parameter essentially depends on the quality of the reflecting surfaces or the transmissive medium (air or glass) encountered between the separation and combination of the science beam. Any configuration limiting the number of surfaces or the length of the cavity (if operated in the presence of air) is favoured. The other parameters impact on modulation efficiency varies strongly depending on the configuration. Fourier transform spectrometers, even imaging versions, are fairly common outside the field of astronomy and are found commercially for over 30 years now. The

designs have generally evolved towards the most efficient and reliable architectures over time due to the strong competition between industrial players. Cube corner retro-reflector-based interferometers are by far the most common architecture found in both single pixel and imaging systems nowadays. The reason for this is that they are inherently tilt errors free (item #2) as long as their three mirror surfaces remain orthogonal to one another to the same precision as is acceptable for the tilt error. Cube corners of acceptable quality for infrared interferometry down to 1 um are found commercially in sizes up to 5 cm. The problem is that SITELLE would require cubes with four times better alignment and reflected wavefront errors in size exceeding 20 cm of clear aperture. Moreover, cube corner retroreflectors behave notably badly with temperature such that most systems are temperature-stabilised to maintain the best performance. We wish to operate SITELLE at ambient temperature given that it will be mounted directly on the telescope and that stringent heat dissipation requirement must be met in the dome environment. Our search of potential supplier rapidly concluded to a risky endeavour if at all possible for SITELLE's available budget. Inability to achieve the required performance would result in irrecoverable performance losses at short wavelengths.

Considering this, we looked more carefully into the more classical flat mirror Michelson original design. In addition to using simple optical components (plane mirrors) readily available commercially, this approach removes two reflecting surfaces which helps to further reduce the errors between recombining wavefronts. The plane mirror architecture also does not create shears between recombining wavefronts. Its drawback is that a dynamic alignment system must be implemented to correct for the followings contributors:

- Residual tilt at interferometer integration;
- Tilt induced by thermal distortion over the operating range (interferometer follows ambient);
- Tilt induced by the varying instrument orientation due to the Cassegrain mounting;
- Inherent tilt profile of the scan mechanism.

Contrary to the large high quality cube corner, tip-tilt mechanisms with precision down to the arc second are now common in astronomy thanks to adaptive optics. ABB also has a vast heritage in dynamically aligned plane mirror interferometers, since it carried a high resolution commercial spectrometer for more than 20 years based on that technology. Also, the first dynamically aligned plane mirror interferometer to fly in space in 2011 was produced by ABB based on that same technology platform[9].

The only remaining issue is how to separate the second output port from its input. In a plane mirror interferometer, half of the light goes to one output and the other half is retro-reflected on itself toward the target. This is not acceptable in ground-based astronomy since the sky transparency may affect the source intensity during the scanning of the OPD. The Fourier transform operation finds the associated spectral content for all intensity variations present in the input vector and makes no distinction between true interference and undesired source fluctuation. The access to the second input port is crucial in being able to compensate for the source variation before performing the Fourier transform.

To overcome this problem, the solution already implemented in SpIOMM was reused (see Figure 2). It consists of entering the interferometer at a given angle such that the coincident output is angularly separated from the input. The angle is made just large enough to locate the collimator lens and the camera lens barrels side-by-side as depicted in the simplified diagram below.

The sketch below showing the whole layout in a 2D plane results in a rather large beamsplitter footprint. A more compact approach is obtained by entering the input beam in a plane perpendicular to the one shown (off-axis input/output rotated at 90 degrees to the interferometer plane). Another advantage of the dual output flat mirror configuration with respect to the cube-corner one is that it results in a much smaller moving mass. A dual output port cube corner interferometer is obtained by entering the science beam in the lower half part of the cube corner which translates it to its upper half. The clear aperture size required for the cube more than doubles the pupil size given that sufficient clearance must be generated in the lateral transfer to account for beam divergence and the longitudinal distance to reach the beamsplitter. A higher moving mass means lower resonance modes and a lower frequency response of the OPD servo system.

The SITELLE interferometer final design based on this architecture is shown in Figure 3.

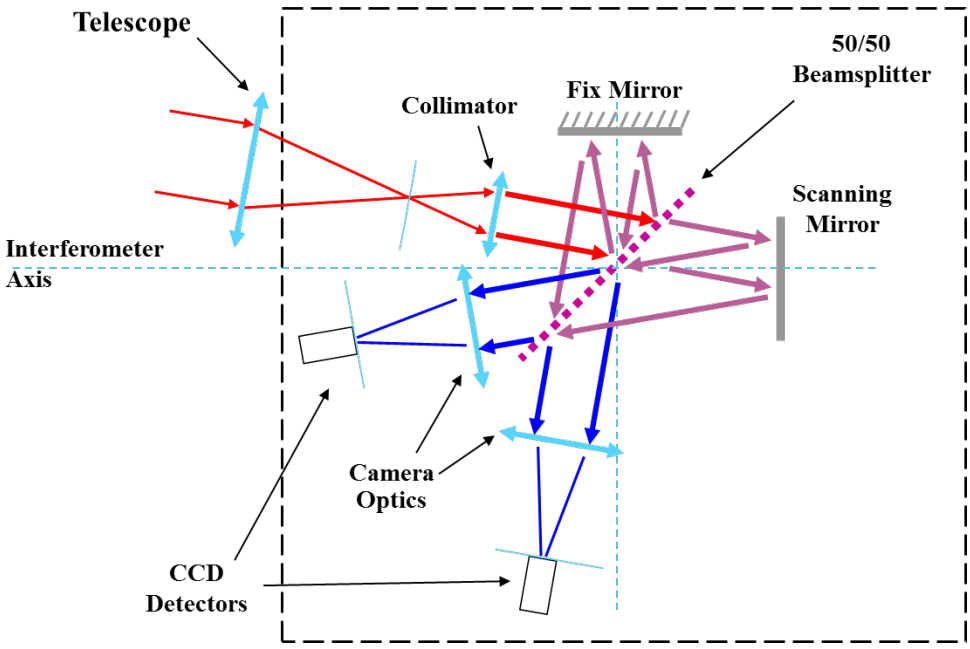

Fig. 2 - Simplified representation of the optical arrangement of SITELLE

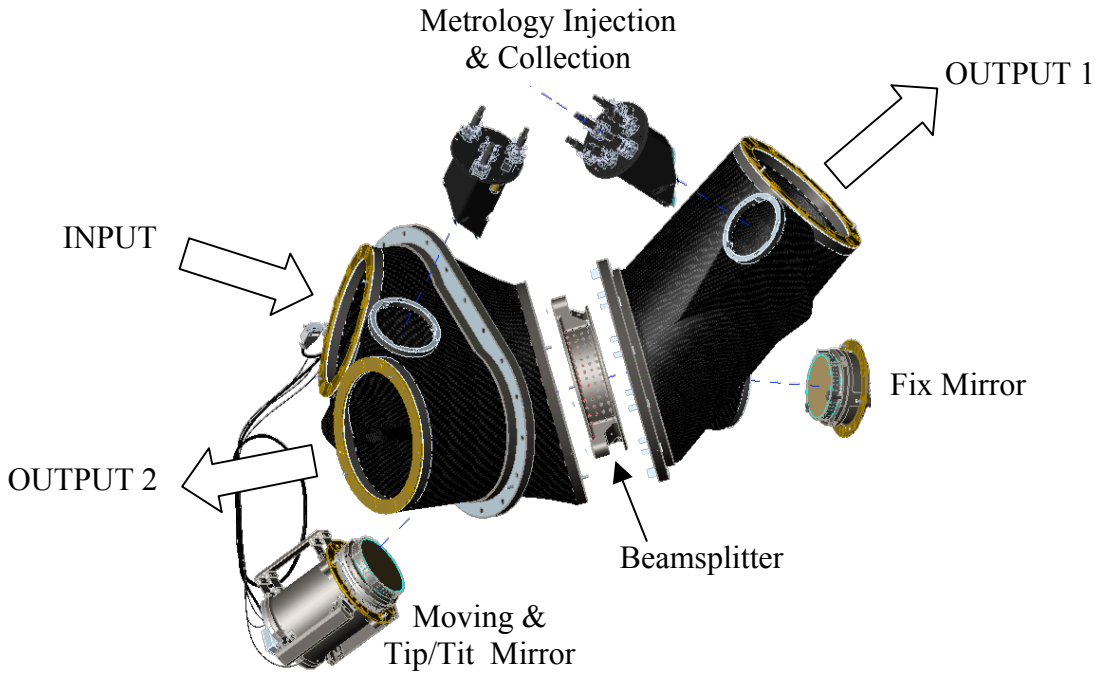

Fig. 3 - Exploded view of the interferometer structure

The beamsplitter is a key driver in the instrument performance. For SITELLE, we chose a sandwich-type configuration which has the splitting coating sitting in the middle of two identical glass substrates. This ensures identical optical paths in both arms and prevents the wavelength dispersion of the zero path difference (ZPD). This part is made by optically contacting the two substrates, one of which is pre-coated with a multi-layer dielectric coating carefully tailored to the SITELLE spectral range as shown in Figure 4. The thickness and complexity of the coating is traded to offer a good performance while minimizing thermal stress induced on the substrate and impact on the wavelength dispersion of the ZPD which affect the performance of the interferogram asymmetry corrections. The coating averages around 60% and 40% for the reflectivity (R) and the transmission (T) such as leading to a modulation efficiency contribution around 96% across the visible band. The final assembly is checked for reflected and transmitted wavefront errors and is corrected by ion beam figuring in order to yield the best possible flatness. The aspect ratio of the beamsplitter is chosen to be very robust with 8:1 on the individual substrates and 4:1 on the ensemble. Broadband AR coating are applied on both external faces of the splitter. The sandwich beamsplitter approach aims to correct an anomaly noted in SpIOMM which had and air gap-spaced compensator plate. The angle between the compensator plate and the beamsplitter was changing slightly (few arc seconds) with respect to the beamsplitter with instrument pointing angle. This created a moving ghost on the images of the cubes proportional in intensity to the performance of the AR coating.

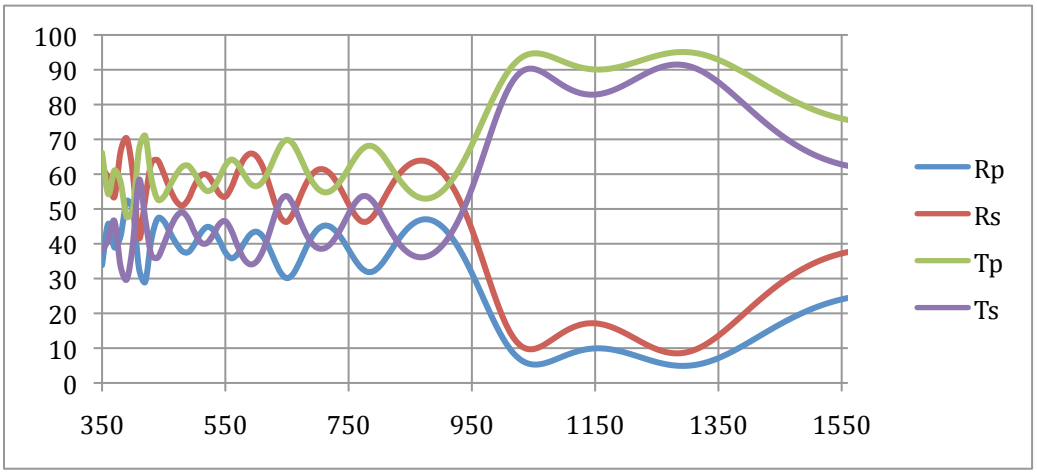

Fig. 4 - Intereferometer beamsplitter coating's expected performance

The scan mechanism is a custom-designed architecture based on ABB's heritage in flex-blade actuated frictionless scan mechanism. The blades arrangement surrounding the mechanism produces a purely translational movement and reduces tilt sensitivity to gravity orientation changes with a first tilt mode at 540 Hz. It is actuated by piezos. A PI Nexline is used for the coarse displacement and stack piezos are used for fine tuning of the OPD and the alignment. The absence of static friction combined with the piezos allows for sub-nm OPD corrections. The flex blades are actuated below the fatigue limit of the material within the scanning range so the mechanism can operate without degradation for millions of cycles. The high axial rigidity produced by the Nexline actuator and the piezos stack also reduces sensitivity to operational vibration by ensuring the moving mirror follows the rest of the interferometer movement if present.

The metrology uses a 1550 nm high stability laser. The CCD detector is not sensitive to the laser wavelength, which allows to constantly monitor and correct OPD and alignment during exposure of the detector. A multi beam pattern surrounding the science beam allows to easily retrieve both mirror position and angle with a precision better than 1/1000th of a laser fringe. The metrology fringe signals are digitized by an ADC and processed using an ABB proprietary method based on quadrature fringe signal which provides continuous absolute OPD information throughout the 1 cm scanning range at a frequency of 10 kHz. The metrology servo does not require such a high sampling rate to operate but the feedback is meant to be very rapid to ensure proper safety margin between successive readings to avoid confusion between adjacent fringes under rapid perturbations.

3.3 The instrument structure

The interferometer is the structure onto which the collimator barrels and the two camera assemblies are fixed. With these in place, the interferometer cavity is a sealed enclosure which prevents air fluctuation and allows for dry purging. This rigid optical train is then fixed near its center of gravity (located within the interferometer enclosure) to the telescope using a two-layer thrust architecture as shown in Figure 5. The two layers approach provides a more rigid structure than a single long thrust design and has the advantage of offering a middle plate to fix the filter wheel and the calibration target wheel in front of the collimator near the telescope focal plane. The thrusts are made of carbon fiber and their pattern and shape are customized to meet the instrument flexure requirement which shall remain below 2 pixels throughout all possible instrument orientations and temperatures of operation. The annular plates holding the thrusts are weight relieved from the inside to further reduce the mass of the instrument which amounts to 340 kg. The overall dimensions of the instrument are 2.3 x 1.8 x 1.8 meters. A neoprene blanket (not shown on the picture) covers the instrument for further protection of the instrument components against the harsh telescope environment. The camera controllers are mounted directly to the SITELLE structure in order to minimize the noise associated with cable length. The rest of the SITELLE electronic components sits in a separate electronics box mounted on a fixation site surrounding the telescope mirror. The elements contained in the electronics box and the interconnections between the various SITELLE elements are highlighted in the block diagram shown in Figure 6 along with the distribution of the responsibility among the partners.

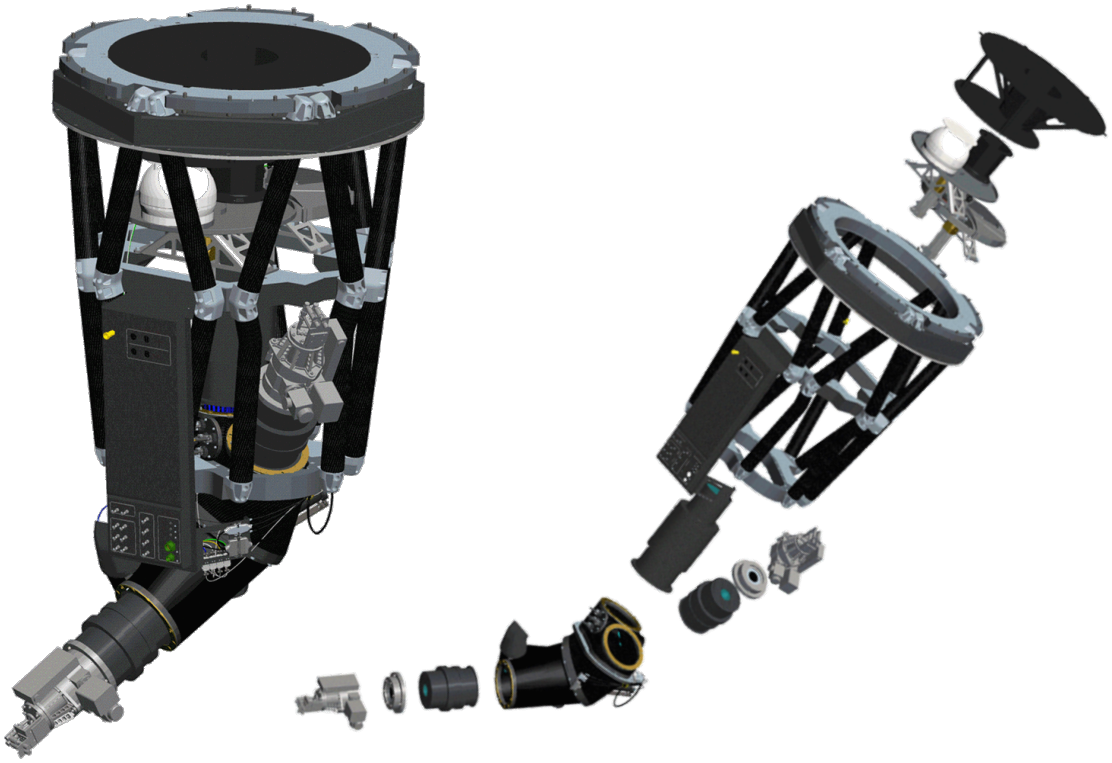

Fig. 5 SITELLE assembled (left) and exploded (right) views

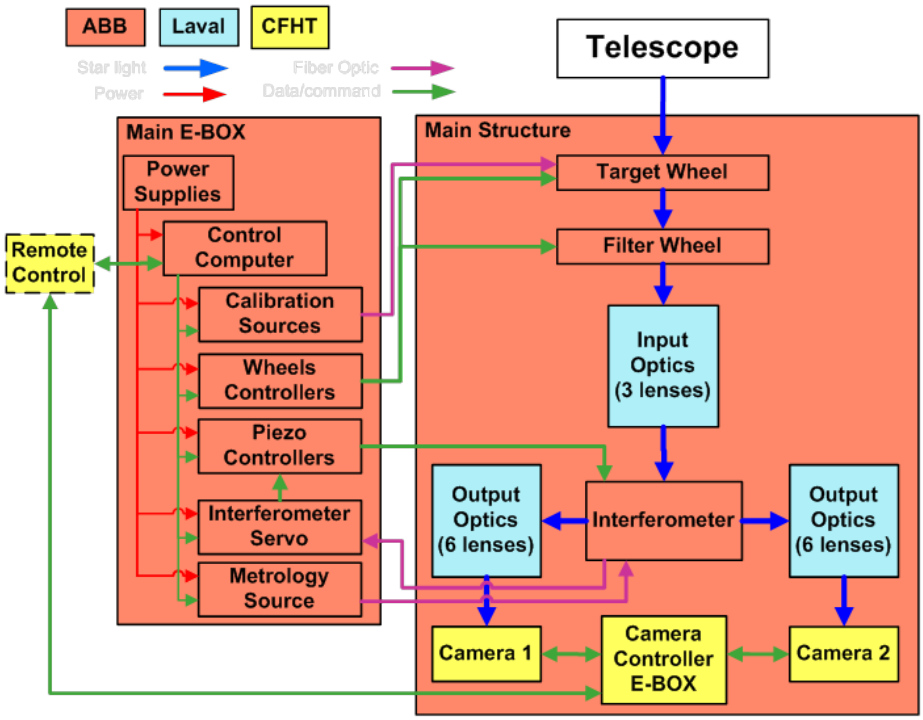

Fig. 6 SITELLE bloc diagram

3.4 Detector

As with all astronomical instruments, the detector is a critical component of the system. In the case of an imaging FTS, two characteristics are especially important. As the spectra acquisition requires numerous images (nominally slightly more there are spectral points to populate) compared to a single exposure grating-based spectrometer, the readout time and noise have a stronger negative impact. Hence, the total readout time ideally represents a negligible fraction of the on-target exposure time. For a given spectral resolution and range, thus fixing the number of images to acquire, the total on target integration time will determine the SNR of the spectra and consequently each image exposure time. This calculation typically leads to exposure times per step ranging from 10 seconds to one minute for the science cases outlined at the beginning of this paper. A one second read time can thus lead to up to 10% loss of observing efficiency. Unfortunately, such read rate or faster come at the expense of a rather large read noise which significantly reduces the overall sensitivity of the instrument. Hence a compromise is sought.

For SITELLE, we decided to use a four output 2 k x 2k low noise e2v chip that allows attaining 5e noise in 1 second read time and 3.5 electron in 2 seconds. These values are reasonably small and allow for sufficient time to move and stabilize the interferometer mirror while the camera shutter is closed. The selected CCD231-42 e2v chips also allow for high quantum efficiency in the near UV below 400 nm. When used with the Astro wide-band coatings, a quantum efficiency of 65% is obtained at 370 nm below the [OII] 372.7 nm line.

No vendor currently offers this detector packaged in a dewar with noise matched readout electronics. This task was thus undertaken by the CFHT. The custom nature of the dewar assembly also allowed to address another issue particular to the IFTS; the vibrations. The CFHT now operates fully remotely from the base of the mountain in Waimea and their preferred detector cooling system is based on closed cycled pumped gas cryogen (Polycold System's Cryotiger). Those systems generate vibrations on the cooling lines that are communicated directly to the dewar and chip assembly which must be rigidly mounted to the interferometer. Those vibrations were characterized experimentally and present a complex spectrum which span over a large frequency range (Baril et al., these proceedings). The interferometer servo is meant to compensate perturbations with frequencies typically below 100 Hz. Perturbations above this will affect the OPD stability and hence the modulation efficiency. To overcome this, a special vibration-isolated dewar was designed

using a two section design coupled with sorbothane rings. The conduction to the chip is assured through flexible strap (see Figure 7).

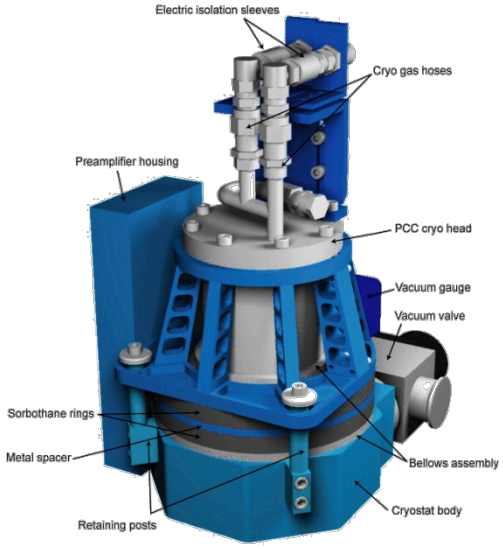

Fig. 7 Detector assembly

4. EXPECTED PERFORMANCE

Great expectations are set for SITELLE. The interferometer configuration inherently offers the potential for attaining high spectral resolutions, although the chosen off-axis configuration and the imaging nature of the instrument somewhat precludes working at very high resolutions (10^5 or more). Nevertheless, the off-axis resolution limitations are matched to the scanning range such that the required resolutions (see Figure 8) can be expected when using the full stroke of the mirror. In Figure 8, the region in yellow shows that the resolution requirement set by the science objectives was largely exceeded due to the simplicity to extend the stroke of the scan mechanism even though few programs if any will be using this regime of the instrument. Moreover, in this region, the off-axis configuration creates a gradient in the spectral resolution obtained across the array. The pixel running the closest to the interferometer axis is the least affected and the two corner pixels away from the axis are the most affected by a phenomenon known as “self apodisation” of the interferogram that is caused by the interference fringes in the images becoming as small as the pixel themselves at large OPD. The coarsely spatially sampled interference fringes result in a reduction of the perceived modulation efficiency. The green curves superposed to the graph and tied to the right axis show the wavelength dependence of the modulation efficiency observed at the maximum OPD (end of mirror stroke) for a detector binned 2x2 pixels (0.64 arcsecond). The resolution curve are also produced for the same binning, which is more representative of reality given the seeing extend roughly over 4 pixels. It can also be noted from this graph that an FTS produces a spectral resolution which is constant in frequency but increases non-linearly with decreasing wavelengths.

The other critical performance parameter of the instrument is the overall instrument efficiency. We already touched on the temporal observing efficiency, but we now reporting on the overall efficiency with all detector shutters open, a combination of the overall transmittance of the instrument and the expected modulation efficiency from the beamsplitter coating and the other parameter mentioned in the previous section. Figure 9 shows the current best estimates assuming AR coating performance of less than 1% on all optics of the instrument train. This performance has yet to be demonstrated experimentally but the servo sensitivity, the FEM analysis of all instrument parameters, were selected to meet this value. Such a high value for a spectrograph is only attainable due to the relatively small number of optical components and the very careful design of the interferometer module. As always with interferometry, the shortest waves

are the most at risk but it is our perception that the final curve may be more affected by actual coating performance than by the interferometer itself.

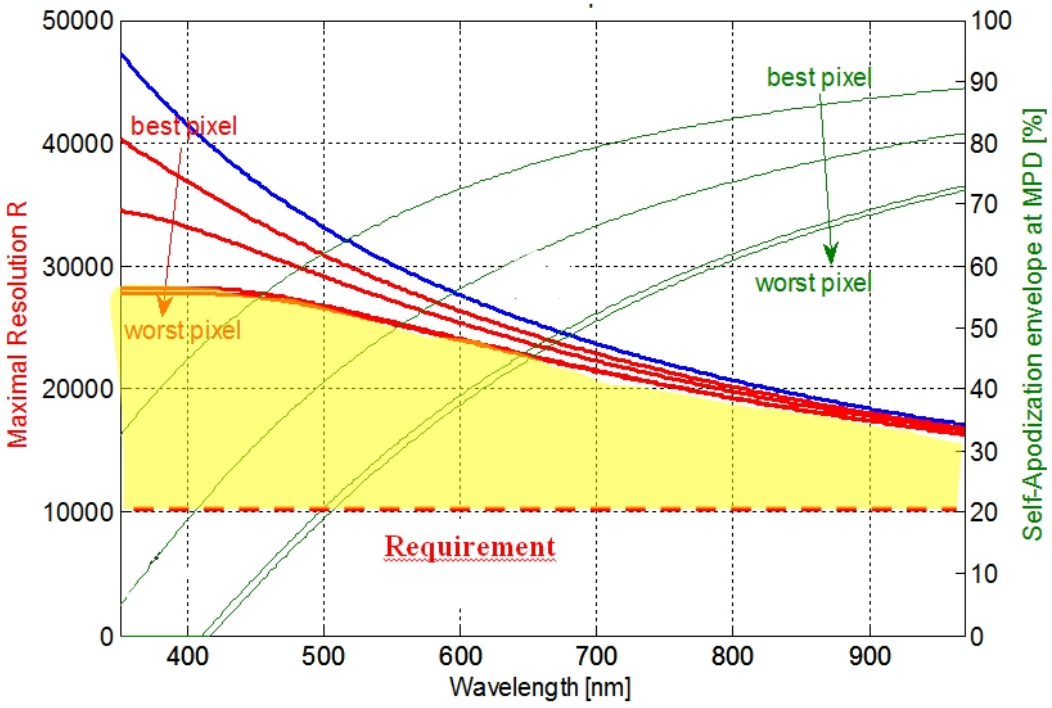

Fig. 8 - Maximum spectral resolution expected from SITELLE as a function of wavelength

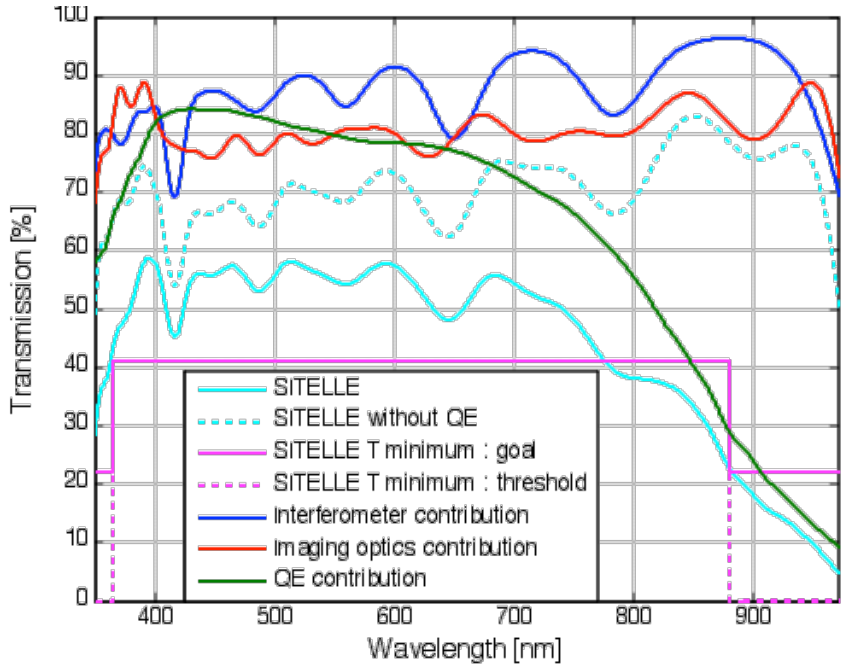

Fig. 9 - Overall throughput of SITELLE with the contributions from its individual components

5. CONCLUSION

SITELLEis the result of a 12 year collaboration between Université Laval and ABB, which started following an ABB-HIA proposal for a similar instrument on the JWST back in 1999. The Mégantic 1.6-meter SpIOMM prototype IFTS which followed saw its first light in 2004 and was a key development step for SITELLE. SpIOMM allowed to demonstrate the feasibility, readiness and true potential of the concept which led to the acceptance of the SITELLE proposal by CFHT. SITELLE will be the first wide-field imaging FTS operating in the visible range on a large optical telescope and will set a performance benchmark for experimental comparisons with other type of IFUs in terms of SNR and data quality. SITELLE offers capabilities that no other instrument can pretend to and as such it should allow for very promising new science!

ACKNOWLEDGEMENTS

We acknowledge funding by the Canadian Foundation for Innovation, e2v, CFHT, ABB, NSERC (Canada), FQRNT (Québec) and Université Laval.

REFERENCES

[1] Grandmont, F., Drissen, L., & Joncas, G. , Proc. SPIE, 4842, 392 (2003)
[2] Bernier, A.-P., Grandmont, F., Rochon, J.-F.. Charlebois, M., & Drissen, L. , Proc. SPIE, 6269, 135 (2006)
[3] Drissen, L., Bernier, A. -P., Charlebois, M., Brière, É., Robert, C., Joncas, G., Martin, P., & Grandmont, F. , Proc. SPIE, 7014, 70147K (2008)
[4] Bernier, A. -P., Charlebois, M., Drissen, L., & Grandmont, F. , Proc. SPIE, 7014, 70147J (2008)
[5] Drissen, L., Bernier, A.-P., Rousseau-Nepton, L., Alarie, A., Robert, C., Joncas, G., Grandmont, F., Thibault, S. SPIE, 7735, 77350B (2010)
[6] Ridgway, S. T. & Brault, J. W. 1984, Ann. Rev. Astron. Astrop. 22, 291
[7] Bennett, C. L. 2000, in *Imaging the Universe in Three Dimensions*, ASP Conf. Ser. Vol 195, p. 58
[8] Maillard, J.-P., Drissen, L., Grandmont, F., & Thibault, S., submitted to Experimental Astronomy (2012)
[9] Glumb, R. J., Jordan, D. C., & Mantica, P., Proc. SPIE, 4486, 411 (2002)